

High-sensitivity high-resolution sampling using linear optics and waveguide optical hybrid

C. Dorrer, C. R. Doerr, I. Kang, R. Ryf and P.J. Winzer
 Bell Laboratories-Lucent Technologies, 101 Crawfords Corner Road, Holmdel, NJ, 07733, USA
 Phone: 732 332 6463, Fax: 732 949 2473, email: dorrer@lucent.com

Abstract: A practical sampling setup based on linear interference of an optical signal with a sampling pulse in a waveguide optical hybrid demonstrates record-sensitivity sampling of eye diagrams up to 640 Gb/s with high fidelity.

©2004 Optical Society of America

OCIS codes: (130.1750) Components, (320.7160) Ultrafast technology.

1. Introduction

Sampling techniques allow the monitoring of optical signals used in optical telecommunications, via a statistical representation such as an eye diagram. While all-electronic detection and sampling are sufficient at rates of 40 Gb/s and below, higher bit-rates require optical implementations of temporal gates such as a nonlinear interaction with a short optical pulse. The time resolution of nonlinear optical sampling is limited only by the response of nonlinear interaction, phase-matching conditions and the bandwidth of the short sampling pulse [1-5]. However it usually lacks sensitivity, and sampling at 500 Gb/s and 640 Gb/s were achieved with sensitivities of 10^6 mW^2 and 10^8 mW^2 , calculated as the product of the peak power of the two sources, using cross-phase modulation in a highly nonlinear fiber and sum-frequency generation in a PPLN crystal respectively [4,5]. In linear optical sampling, highly sensitive temporal characterization is obtained using two orthogonal quadratures of the linear interference of the electric field of the waveform under test with the electric field of the sampling pulse [6]. Such a concept was demonstrated at 80 Gb/s using a free-space setup.

We demonstrate a new implementation of linear sampling based on a silica-waveguide optical hybrid that combines the electric fields appropriately, optimizes the relative phase between the two quadratures of their interferometric component and has high practicality compared to the free-space setup. Thanks to the linearity of the diagnostic, the bandwidth is only limited by the bandwidth of the sampling pulse. Moreover, high sensitivity can be obtained and data waveforms can be reproduced without distortion by optimization of the sampling pulse. Eye-diagram measurements at 640 Gb/s with record sensitivity of $3 \cdot 10^3 \text{ mW}^2$ are demonstrated.

2. Concept of linear optical sampling

Linear optical sampling measures samples of the source under test using two orthogonal quadratures of the interference of its electric field E_D with that of a train of sampling pulses $\sum E_{S,N}(t-NT)$ [6]. Optically coupling the two sources and performing time-integrating balanced detection of the two outputs leads to:

$$S_{A,N} = \text{real} \left[\exp(i\varphi_A) \cdot \int E_D(t) \cdot E_{S,N}^*(t-NT) dt \right] \quad (1)$$

where φ_A is a phase difference related to the path length between splitters and combiners. As the value of such a quadrature is highly dependent on the phase of the two sources, one simultaneously measures an orthogonal quadrature:

$$S_{B,N} = \text{real} \left[\exp(i\varphi_B) \cdot \int E_D(t) \cdot E_{S,N}^*(t-NT) dt \right] \quad (2)$$

where $\varphi_B - \varphi_A = \pm\pi/2$. $S_{A,N}$ and $S_{B,N}$ are squared and summed to yield:

$$S_N = \left| \int E_D(t) \cdot E_{S,N}^*(t-NT) dt \right|^2 = \left| \int E_D(\omega) \cdot E_{S,N}^*(\omega) \cdot \exp(iN\omega T) d\omega \right|^2 \quad (3)$$

where ω is the optical frequency. Following Eq. 3, if the sampling pulse has flat spectral density and phase over the range of optical frequencies where the source under test has significant spectral density, the samples simplify to $S_N = |E_D(NT)|^2$, which means the diagnostic provides the instantaneous value of the temporal intensity of the source under test, without distortion or resolution limitation. Additionally, Eq. 3 shows that only the photons

of the sampling source that spectrally overlap with the source under test participate in the sampling process. Therefore, the sampling source can be optimized spectrally in order to provide optimal resolution and sensitivity.

3. Implementation of linear optical sampling using 90°-waveguide optical hybrid

The first linear optical sampling diagnostic used a free-space setup to combine the two sources and generate the linear combinations corresponding to Eqs 1 and 2 via polarizers and waveplates. Such operations can be performed advantageously with a 90° optical hybrid based on silica waveguides on a silicon substrate (Fig. 1 and 2). Such a structure is wavelength and polarization insensitive. The phase of one of the arms of the hybrid can be adjusted using a voltage applied to a thermo-optic phase shifter (a voltage of 3 V corresponds to a phase shift of about one radian), so that the relative phase between the interfering fields of Eqs. 1 and 2 is $\pm \pi/2$. The connector-to-connector input-to-output losses measured using a non-polarized source range from 9.5 dB to 10.1 dB, including 6 dB corresponding to the power splitting. The polarization dependent loss was measured to be 0.6 dB.



Fig. 1. 90° waveguide optical hybrid (left). The sources are input on the left, split and recombined into 4 outputs on the right. The relative phase between the two quadratures can be set using a thermo-optic phase shifter, and examples of quadratures measured for phase differences equal to 0, $\pm \pi/2$ and π are plotted on the right.

The silica-hybrid accepts the copolarized sampling source and source under test as 2 inputs and combines them as 4 outputs on which balanced detection is performed with the 700 MHz detectors BDA and BDB (Fig. 2). An analog-to-digital sampling board simultaneously acquires the two quadratures, which are then processed to yield the samples corresponding to Eq. 3. The sampling pulse, which has initially significant spectral density over 40 nm, is spectrally filtered in order to match its spectral density to that of the source under test. Gaussian-shaped filters were used below 160 Gb/s. To accommodate the larger bandwidth of pulses in the 1 ps range, the sampling laser was filtered using a free-space grating-based filter that provides a rectangular pass-band filter. This optimizes the resolution and sensitivity, following Eq. 3.

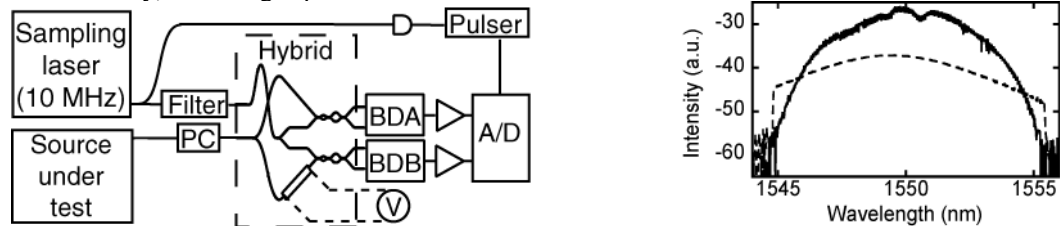


Fig. 2. Implementation of linear optical sampling with the waveguide optical hybrid of Fig. 1a (left) and spectral density of the source under test at 640 Gb/s (continuous line) compared to the spectral density of the sampling pulse after filtering in a free-space grating-based filter (dashed line).

4. Experimental results

The waveguide implementation was first tested on 33 % RZ 10 Gb/s signals generated using a LiNbO₃ Mach-Zehnder modulator (MZM) pulse carver and LiNbO₃ MZM data modulator. The eye diagrams measured for a sampling peak power of 50 mW and data average power of -20 dBm and -30 dBm (i.e. peak powers of 60 μ W and 6 μ W) are plotted in Fig. 3. This indicates a sensitivity of the order of 1 mW^2 at 10 Gb/s, which is of the order of 10 times better than the free-space implementation.

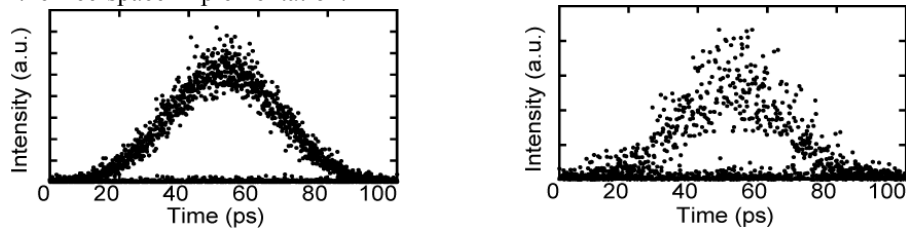


Fig. 3. 10 Gb/s eye diagrams measured at peak signal powers equal to 60 μ W (left) and 6 μ W (right).

Eye diagrams were then measured for amplitude-shift-keyed 2.4 ps pulses from an actively mode-locked source multiplexed up to 160 Gb/s (Fig. 4). The peak power of the sampling pulse was 1.2 W, and the diagnostic easily characterizes 160 Gb/s signals with a peak power of only 50 μ W, leading to a sensitivity of the order of 60 mW^2 .

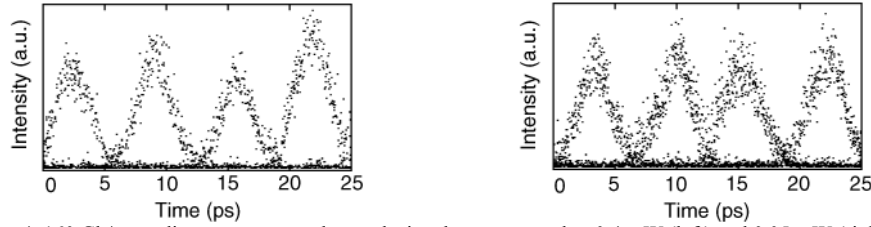


Fig. 4. 160 Gb/s eye diagrams measured at peak signal powers equal to 0.4 mW (left) and 0.05 mW (right).

The 2.4 ps pulses were then compressed to 1.2 ps with a combination of self-phase modulation and chromatic dispersion. The sampling pulse was filtered with a grating-based filter to optimize the resolution and sensitivity according to Eq. 3, as was displayed on Fig. 2. A test of the resolution of such diagnostic was implemented by comparing the second order intensity autocorrelation of the 1.2 ps pulse measured with a standard second order intensity autocorrelator to the second-order intensity autocorrelation calculated from the temporal intensity measured by the diagnostic (Fig. 5). An excellent agreement between the 2 autocorrelations shows that minimal distortion is introduced by the sampling setup. The full-width at half-maximum of the calculated and measured autocorrelations are respectively 1.72 ps and 1.54 ps, which shows that the diagnostic has a very small (of no practical importance) time blurring due to bandwidth limitation and jitter. Eye diagrams of the 1.2 ps pulse were measured for amplitude-shift-keyed modulation at 10 Gb/s and after time-multiplexing up to 640 Gb/s (Fig. 6). The sensitivity in this case is equal to 3.10^3 mW^2 , calculated as the product of the peak powers of the two sources.

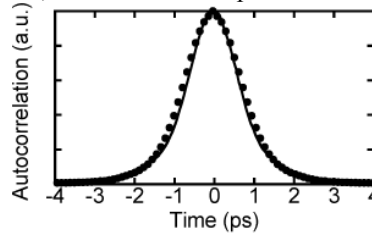


Fig. 5: Second-order intensity autocorrelation calculated from the intensity sampled by the linear sampling diagnostic (markers) and independently measured by an autocorrelator (continuous line).

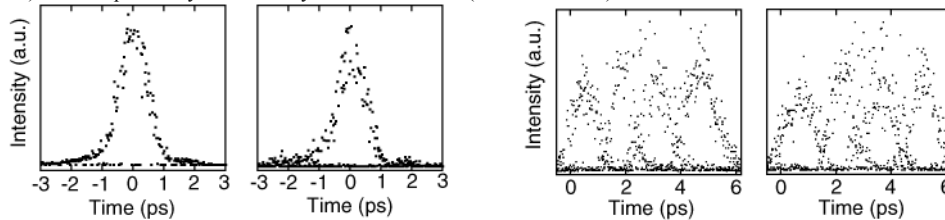


Fig. 6. 10 Gb/s eye diagrams of the 1.2 ps-pulse at peak signal powers of 16 mW and 0.6 mW (left) and 640 Gb/s eye diagrams of the 1.2 ps pulse at peak signal powers of 2.5 mW and 0.6 mW (right). In both cases, the peak power of the sampling pulse is 5 W.

5. Conclusion

The first implementation of linear optical sampling using an integrated waveguide optical hybrid allows the measurement of eye diagrams up to 640 Gb/s with record sensitivity and excellent time resolution. As no nonlinear interaction is involved, implementation for characterizing even shorter pulses requires only a shorter sampling pulse.

- [1] J. Li, J. Hansryd, P. O. Hedekvist, P. A. Andrekson, and S. N. Knudsen, "300-Gb/s eye-diagram measurement by optical sampling using fiber-based parametric amplification," *IEEE Photon. Technol. Lett.*, vol. 13, pp. 987-989, 2001.
- [2] H. Ohta, N. Banjo, N. Yamada, S. Nogiwa and Y. Yanagisawa, "Measuring eye diagram of 320 Gb/s optical signal by optical sampling using passively modelocked fibre laser," *Electron. Lett.*, vol. 37, pp. 1541-1542, 2001.
- [3] I. Kang and K. F. Dreyer, "Sensitive 320 Gbit/s eye diagram measurements via optical sampling with semiconductor optical amplifier-ultrafast nonlinear interferometer," *Electron. Lett.*, vol. 39, pp. 1081-1083, 2003.
- [4] J. Li, M. Westlund, H. Sunnerud, B-E. Olsson, M. Karlsson, and P. A. Andrekson, "0.5 Tbit/s eye-diagram measurement by optical sampling using XPM-induced wavelength shifting in highly nonlinear fiber," *Mo 4.6.4, European Conference on Optical Communication*, 2003.
- [5] N. Yamada, S. Nogiwa, and H. Ohta, "Measuring eye diagram of 640-Gbit/s OTDM signal with optical sampling system by using wavelength-tunable soliton pulse," *Mo 4.6.5, European Conference on Optical Communication*, 2003.
- [6] C. Dorrer, D. C. Kilper, H. R. Stuart, G. Raybon and M. G. Raymer, "Linear optical sampling", *Photon. Technol. Lett.* **15**, 1746-1748 (2003).